*Proc. Natl. Acad. Sci. USA*
Vol. 94, pp. 2975–2980, April 1997
Biochemistry

# Crystal structure of desheptapeptide(B24–B30)insulin at 1.6 Å resolution: Implications for receptor binding

SU-JIN BAO, DIAN-LIN XIE, JI-PING ZHANG, WEN-RUI CHANG, AND DONG-CAI LIANG*

National Laboratory of Biomacromolecules, Institute of Biophysics, Chinese Academy of Sciences, Beijing 100101, China

*Communicated by John Kendrew, University of Oxford, Cambridge, United Kingdom, January 13, 1997 (received for review July 1, 1996)*

**ABSTRACT** **The crystal structure of desheptapeptide (B24–B30) insulin (DHPI), a virtually inactive analog of insulin, was determined at 1.6 Å resolution. In the refined structure model, DHPI retains three α-helices (A1–A8, A12–A18, and B9–B19) as its structural framework, while great conformational changes occur in the N and C termini of B-chain. The β-turn, which lies in B20–B30 in insulin and insulin analogs with high potency, no longer exists in DHPI. Relative motion is observed among the three α-helices, each as a rigid functional group. In contrast, a region covering B5–B6 and A6–A11 exhibits a relatively stable conformation. We interpret our results as identifying: (*i*) the importance of β-turn in determining the receptor-binding potency of insulin and (*ii*) a leading role of Phe$^{B24}$ in maintaining the β-turn structure.**

The C terminus of insulin B-chain is known to be important in the interaction of insulin with its receptor (1–8). Current studies on the character of B24–B25 indicate that these residues may play pivotal roles in determining the receptor-binding potency of insulin (9–14). As insulin can bear the replacement of D-amino acid residues at position B24 (10), it raises a question concerning the concrete role the invariant Phe$^{B24}$ may play in ligand–receptor interaction. Despentapeptide (B26–B30) insulin (DPI), with five residues truncated from the C terminus of insulin B-chain, retains 25.7% of the binding potency in the native insulin. Removal of Phe$^{B25}$ in DPI results in 2.3% potency retention, while further removal of Phe$^{B24}$ results in 0.1% binding activity retention (15). To manifest the role of B-chain C terminus, especially Phe$^{B24}$ and Phe$^{B25}$, a series of investigations have been carried out on the crystal structures of truncated analogs, among which the crystal structures of DPI and deshexapeptide (B25–B30) insulin (DHI) have been determined (16, 17). In this paper, we describe the crystal structure of desheptapeptide (B24–B30) insulin (DHPI), a virtually inactive analog, and compare DHPI with insulin and other insulin analogs. Our studies identify the important role of Phe$^{B24}$ and β-turn (B20–B23) in insulin in directing hormone–receptor interaction.

## MATERIALS AND METHODS

**Crystallization and Data Collection.** DHPI was prepared from porcine DPI by a limited enzymatic method and purified to homogeneity with Sephadex G-50 (18). The single crystals of DHPI were obtained through the use of a sitting drop vapor diffusion method against 0.043 M sodium citrate, 0.1 mg/ml zinc acetate, and 30% (vol/vol) acetone at pH 5.90 (19). The crystals belong to orthogonal space group $P2_12_12_1$. The cell parameters were determined to be: $a$ = 57.40 Å, $b$ = 56.33 Å, and $c$ = 23.03 Å. Crystal density was 1.24 g/cm$^3$, measured using the density gradient of bromobenzene and *p*-dimethylbenzene. This result indicates a molecular mass of 98,500 Da or two DHPI molecules per asymmetric unit. This is consistent with Matthew coefficient $V_m$ of 1.88 Å$^3$/Da and solvent content of 35%, which are within the range typically found in protein crystals (20).

The original data set was collected from two crystals at room temperature using PW 1100 four-circle diffractometer and CuKa radiation from a Rigaku (Tokyo) Ru-200 rotating anode operated at 40 kV and 30 mA. The radiation damage was monitored by measuring 2 reference reflections every hour automatically and another 10 reference reflections equally distributed in different resolution shells every 24 hr. A crystal would be removed if a 10% decrease in its intensities was observed. The correction of absorption was applied by semiempirical method (21), and the diffraction data were processed with PROTEIN (22). A total of 9,523 observations was merged into 5,141 independent reflections (20–2.0 Å) with an $R_{merge}$ of 6.7%. A second data set was collected using the Weissenberg (Tsukuba, Japan) camera system for macromolecules (23) at the beamline BL-6A2 of the Photon Factory synchrotron radiation source in Tsukuba, Japan. The Weissenberg images were read out with a Fuji BAS 2000 scanner. The processing and reduction of the data were performed using the program package WEIS (24). A total of 14,708 observations were collected and merged into 8,171 independent reflections (8–1.6 Å) with an $R_{merge}$ of 7.2%. Finally, the two data sets were merged into a single one. The completeness of this merged data set per resolution shell is shown in Table 1.

**Structure Solution and Refinement.** Molecular replacement using AMORE (25) was carried out with a 1.5 Å structure of DPI (16) in which B24 and B25 were deleted as a search model. The orientations and positions of two independent DHPI molecules in an asymmetric unit were determined with a unique high correlation coefficient of 53.4% in the translation function. The *R*-factor was 40% for all reflection data, ranging from 8 to 3 Å.

The molecular replacement solution of DHPI was the starting model for refinement carried out with X-PLOR (26). Initially, only 3 Å resolution data were included and rigid-body refinement was performed, keeping two DHPI molecules as two rigid bodies. This decreased the *R*-factor to 38.0%. The positional refinement was carried out by means of X-PLOR's energy minimization option, and the x-ray refinement weight was kept at 0.6 times the value recommended by CHECK.INP. The $2F_o-F_c$ and $F_o-F_c$ maps at this stage showed the conformational changes took place in the N- and C-terminal regions of B-chain. To establish the conformation of peptides in these

The publication costs of this article were defrayed in part by page charge payment. This article must therefore be hereby marked "*advertisement*" in accordance with 18 U.S.C. §1734 solely to indicate this fact.


0027-8424/97/942975-6$2.00/0
PNAS is available online at **http://www.pnas.org**.

Abbreviations: DPI, despentapeptide (B26–B30) insulin; DHI, deshexapeptide (B25–B30) insulin; DHPI, desheptapeptide (B24–B30) insulin.

Data deposition: The atomic coordinates have been deposited in the Protein Data Bank, Chemistry Department, Brookhaven National Laboratory, Upton, NY 11973 (reference 1DEI).

*To whom reprint requests should be addressed.

Table 1. Statistics on the merged data set used for the refinement

| Resolution shell, Å | Completeness, % | |
|---|---|---|
| | All data | $\sigma_{cutoff} = 2.0$ |
| 8.0–5.0 | 100.00 | 98.29 |
| 5.0–3.0 | 99.92 | 98.76 |
| 3.0–2.5 | 99.39 | 97.40 |
| 2.5–2.0 | 98.18 | 94.93 |
| 2.0–1.9 | 86.54 | 82.02 |
| 1.9–1.8 | 80.33 | 74.05 |
| 1.8–1.7 | 71.46 | 61.18 |
| 1.7–1.6 | 65.13 | 51.99 |
| **8.0–1.6** | **86.87** | **81.12** |

regions, further refinement calculations were carried out, excluding residues B21–B23 and A21 in both molecules. The overall electron density was quite good, and B21–B23 and A21 could be traced although the densities around these residues were somewhat disordered. The model was rebuilt with FRODO (27), followed by energy minimization. The *R*-factor dropped to 27.5%. The reflection data were extended from 2.5 to 2.0, 1.8, and finally 1.6 Å, gradually, followed by manual adjustment and positional refinement. At the 1.6 Å stage, considering the partially dispersive electron densities of C-terminal B-chains and A-chains compared with those of molecule cores, the occupancies of residues B21–B23 and A21 for both molecules were given <1.0 with 28% of *R*-factor. Finally, the temperature factors were refined, and 85 water molecules (with occupancies of 1.0 for 60 water molecules and 0.7 for the others) were added, with an *R*-factor of 19.6% for 90% of the data between 8 and 1.6 Å and a free *R*-factor of 21.5% for another 10% of the data excluded from the refinement.

**Quality of the Model.** The final model contains 88 residues (residues A1–A21 and B1–B23 for both molecules) and 85

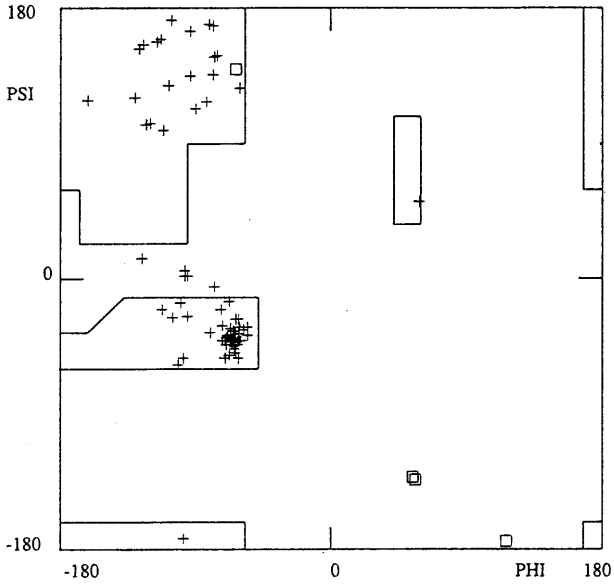


FIG. 2. Ramachandran plot of DHPI structure. Glycine residues are shown as rectangles. [This figure was drawn with the program FRODO (27).]

water molecules. Most of the protein atoms have clear electron density and can be positioned accurately. Representative densities are shown in Fig. 1. The model has a good stereochemistry and the rms deviations for bond length and bond angle are 0.012 Å and 2.75 Å, respectively. No non-glycine residue has energetically unfavorable dihedral angles in the Ramachandran plot, as shown in Fig. 2. The average B-factors are 14.1 Å$^2$ and 30.6 Å$^2$ for protein atoms and water molecules, respectively. Refinement statistics are presented in Table 2. No

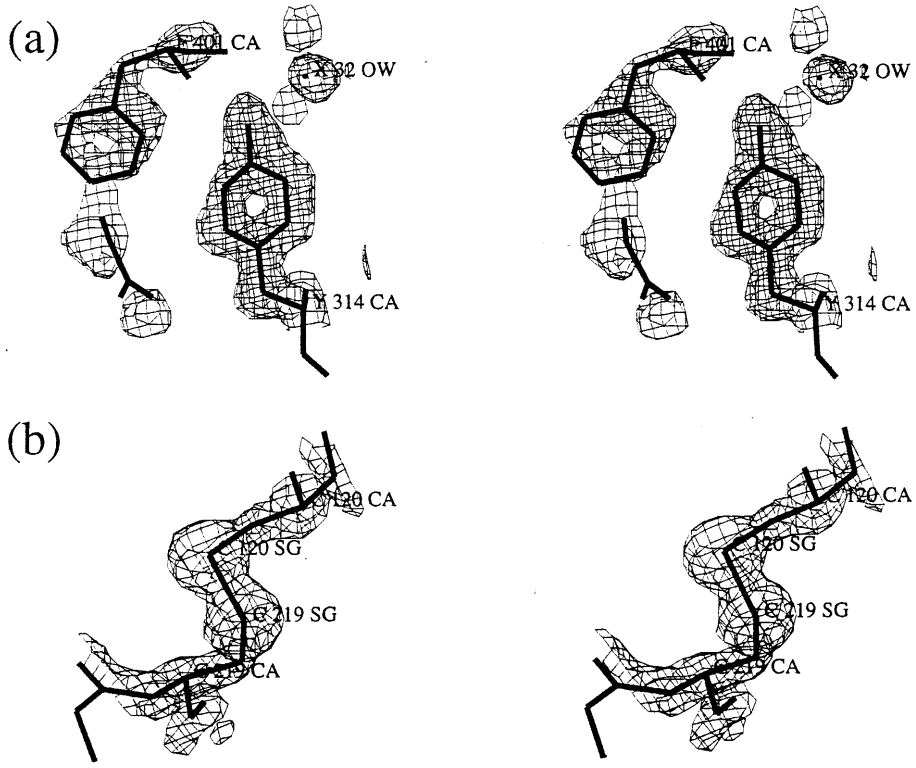


FIG. 1. Representative electron density. The stereoviews show: (*a*) the $2F_o-F_c$ maps of Phe$^{B1}$ of molecule 2 and its nearby area, contoured at 1.0 $\sigma$, and (*b*) the S—S bond between A20 and B19 of molecule 1, contoured at 2.0 $\sigma$. The residues are labeled as follows: A-chain, molecule 1, 101–121; B-chain, molecule 1, 201–223; A-chain, molecule 2, 301–321; and B-chain, molecule 2, 401–423. [This figure was drawn with the program FRODO (27).]

Table 2. Data refinement statistics

| Refinement statistics | Values |
|---|---|
| Resolution range, Å | 8.0–1.6 |
| No. of unique reflections used for the refinement ($F > 2\sigma$) | 8331 |
| No. of protein atoms ($Z > 1$) | 682 |
| No. of water molecules | 85 |
| $R_{cryst.}$,* % | 19.6 |
| $R_{free}$,† % | 21.5 |
| rms deviations from ideal values | |
| Bond lengths, Å | 0.012 |
| Bond angles, ° | 2.75 |
| Dihedral angles, ° | 24.0 |
| Improper angles, ° | 1.56 |
| Average temperature factors, Å$^2$ | |
| Main chain | 12.3 |
| Side chain | 16.5 |
| Solvent | 30.6 |

*$R_{cryst.} = \Sigma|F_{obs}(h) - F_{calc}(h)|/\Sigma F_{obs}(h)$, where $F_{obs}$ and $F_{calc}$ are the observed and calculated structure amplitudes of reflection $h$, respectively. The summation is over all reflections.

†$R_{free}$ is equivalent to $R_{cryst.}$ for a randomly selected 10% subset of reflections excluded from the target set for refinement.

Table 3. The nearest contacts of DHPI

| Contact atoms | Distance, Å |
|---|---|
| 117-Glu-OE2, 209-Ser-CB | 3.20 |
| 221-Glu-OE1, 401-Phe-CB | 3.11 |
| 223-Gly-CA, 401-Phe-CE1 | 3.27 |
| 223-Gly-CA, 401-Phe-CZ | 3.36 |
| 314-Tyr-CE2, 401-Phe-CD1 | 3.29 |
| 314-Tyr-CE2, 401-Phe-CE1 | 3.26 |
| 314-Tyr-OH, 401-Phe-C | 3.29 |
| 104-Glu-CB, 120-Cys-O | 3.38 |
| 108-Thr-OG1, 121-Asn-CB | 3.17 |
| 102-Ile-CG2, 118-Asn-OD1 | 3.26 |
| 105-Gln-OE1, 304-Glu-CB | 3.30 |
| 109-Ser-CB, 310-Ile-O | 3.28 |
| 109-Ser-OG, 305-Gln-CA | 3.25 |
| 109-Ser-OG, 305-Gln-CB | 3.27 |
| 109-Ser-OG, 305-Gln-CG | 3.31 |
| 110-Ile-O, 309-Ser-CB | 3.17 |
| 310-Ile-CD1, 422-Arg-O | 3.23 |
| 405-His-NE2, 423-Gly-CA | 3.38 |

The nearest distances (<3.4 Å) are listed, not including hydrogen bonds. The residues are numbered as follows: A chain, molecule 1, 101–121; B chain, molecule, 201–223; A chain, molecule 2, 301–321; and B chain, molecule 2, 401–423.

close contact is found beyond the range of the typical distances among the van der Waals contacts between DHPI and its symmetry-related molecules (see Table 3).

## RESULTS AND DISCUSSION

**General Structure.** In the refined model of DHPI, each molecule retains three $\alpha$-helices as their structural frameworks corresponding to A1–A8, A12–A18, and B9–B19 in DHPI, as shown in Fig. 3. Great conformational changes take place in the C termini of B-chains for both molecules. The characteristic hydrogen bond between Gly$^{B20}$-O and Gly$^{B23}$-N in 2Zn insulin (29, 30), DPI, or DHI no longer exists in DHPI. The hydrogen bond between Val$^{B18}$-O and Arg$^{B22}$-NH1 or that between Cys$^{B19}$-O and Arg$^{B22}$-N in 2Zn insulin is not found in DHPI either. The torsion angles ($\phi$,$\psi$) of Glu$^{B21}$ and Arg$^{B22}$ turn to be (−90°,114°) and (−162°,119°) in DHPI compared

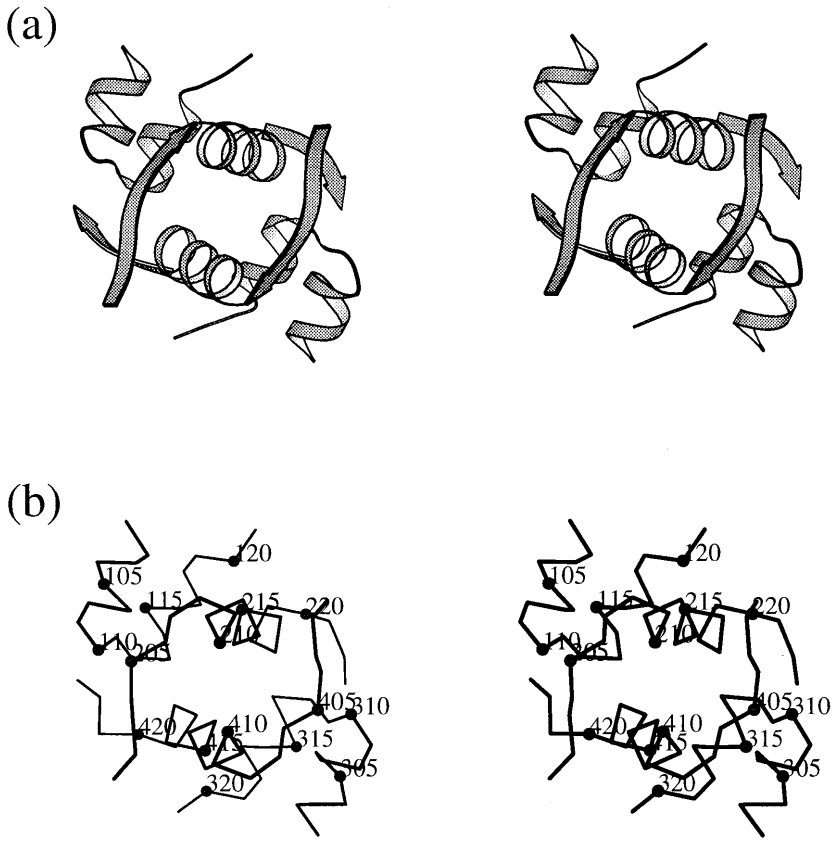


FIG. 3. The overall structure of DHPI. (*a*) A stereo ribbon diagram of DHPI showing view along the local 2-fold axis near (0,0,Z). (*b*) Stereo C$\alpha$ trace of two DHPI molecules, with every fifth residue labeled in each chain. Residues are labeled as in Fig. 1. [This figure was produced using MOLSCRIPT (28).]

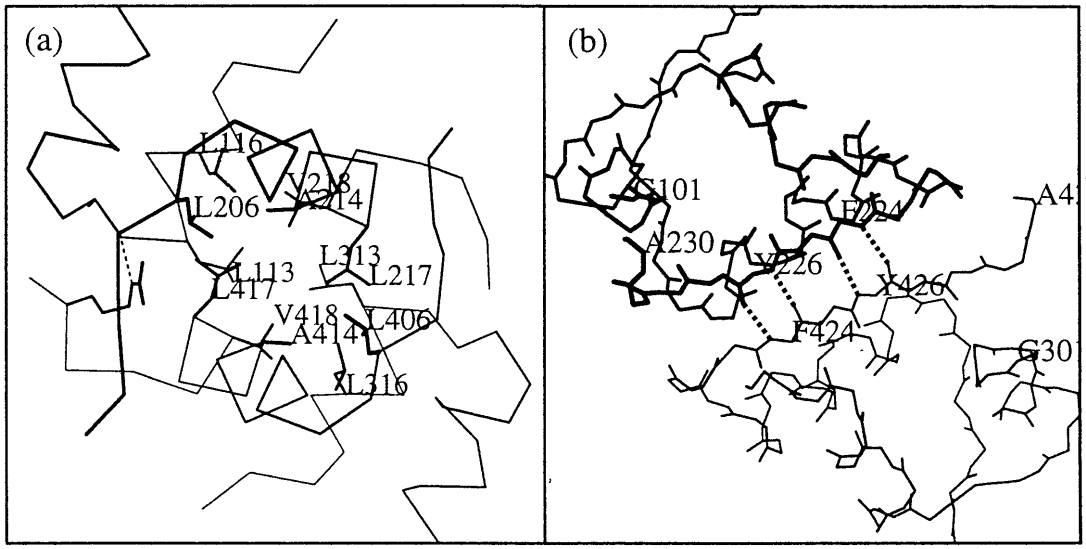


FIG. 4. Contacts of two monomers of DHPI or 2Zn insulin in an asymmetric unit. Molecule 1 of DHPI or 2Zn insulin is shown in boldface while molecule 2 is shown in regular type. (*a*) Contacts through hydrophobic interfaces in two DHPI monomers. The residues involved in the hydrophobic interaction are highlighted in boldface lines. A hydrogen bond linking $Cys^{111}$-O and $Arg^{422}$-NE is shown with a dotted line. (*b*) Contacts through β-strands of C-terminal B-chains in 2Zn insulin dimer. The hydrogen bonds are shown with dotted lines, with bonding residues labeled. Residues are labeled as in Fig. 1. [This figure was produced using MOLSCRIPT (28).]

with (−62°,−24°) and (−68°,−23°) in 2Zn insulin, typical in β-turn structure of proteins. This indicates that DHPI no longer maintains the β-turn in its C terminus of B-chain. Moreover, the low occupancies of B21–B23 (0.4 and 0.6 for molecules 1 and 2, respectively) indicate that these regions exhibit considerably flexible conformation, which is also the case in $Asn^{A21}$. The hydrogen bonds connecting $Asn^{A21}$-N and $Gly^{B23}$-O in 2Zn insulin molecule 1, $Asn^{A21}$-OT–$Arg^{B22}$-NE and $Asn^{A21}$-OT–$Arg^{B22}$-NH2 in 2Zn insulin molecule 2, and $Asn^{A21}$-O–$Arg^{B22}$-NE in DHI are also not found in DHPI. Moreover, the N terminus of B-chain presents the third region with great conformational change compared with 2Zn insulin, DPI, DHI, and des (B1–B2) despentapeptide (B26–B30) insulin (J.-S. Diao and D.-c.L., unpublished data). The average B-factors of B1–B3 are 26.0 $Å^2$ and 25.8 $Å^2$ for molecules 1 and 2, respectively, much higher than the average for the whole molecules (14.3 $Å^2$). Nevertheless, their electron densities are quite clear (Fig. 1).

**Interaction Between Two DHPI Molecules.** A noncrystallographic 2-fold axis is found between the two DHPI molecules in an asymmetric unit after structure solution by molecular replacement. It lies in $(\phi,\psi)$ = (87.5°,78.4°) in the angle system defined by Rossmann and Blow (31) near the crystallographic axis *c*. Shielded by the origin peak at $(\phi,\psi)$ = (90°,90°), the real orientation could not be determined even after several trials in the self-rotation search. Notwithstanding the existence of the local 2-fold axis, interaction of the two molecules differs greatly from that of 2Zn insulin dimer. Instead of contacts through β-strands of C-terminal B-chains as in 2Zn insulin dimer, two DHPI monomers tend to aggregate closely in the asymmetric unit by the hydrophobic interaction through contacts of two hydrophobic interfaces, each composed of $Leu^{A13}$, $Leu^{A16}$, $Leu^{B6}$, $Ala^{B14}$, $Leu^{B17}$, and $Val^{B18}$, as shown in Fig. 4. Forty-three pairs of van der Waals contacts (<3.9 Å) were found between the two monomers in addition to a hydrogen bond (<2.9 Å) between $Cys^{A11}$-O in molecule 1 and $Arg^{B22}$-NE in molecule 2. Moreover, molecule 1 interacts with the symmetry-related molecule of molecule 2 by axis $2_1$ (X,1/4,0) through contacts of A-chains, including 35 pairs of van der Waals contacts (<3.9 Å) and 7 hydrogen bonds (<2.9 Å).

**Comparisons with Insulin and Other Truncated Analogs.** The three α-helices exhibit relatively stable conformation in DHPI as well as in insulin or its truncated forms DPI, DHI and des (B1–B2) despentapeptide (B26–B30) insulin. The rms deviations of main chain superposition of each α-helix of 2Zn insulin and the above analogs are generally <0.3 Å. However, the three α-helices acting as three rigid functional groups are found to take relative motion against each other, and peptide A12–A18 in DHPI has rotated 6.0° and translated 3.6 Å relative to helix B9–B19 as compared with 2Zn insulin (shown in Fig. 5). Nevertheless, the overall structure of the three α-helices in DHPI exhibits a conformational feature much nearer to DHI than to others in their relative displacements (Table 4). Like three α-helices, the disulfide bonds also take motion relative to helix B9–B19. Compared with those of 2Zn insulin, three pairs of S—S bonds, A6–A11, A7–B7, and A20–B19, of DHPI molecule 1 have rotated and translated (2.74°, 0.75 Å), (4.84°, 1.73 Å) and (7.92°, 4.14 Å), respectively (see Fig. 5). As mentioned above, obvious changes occur in the

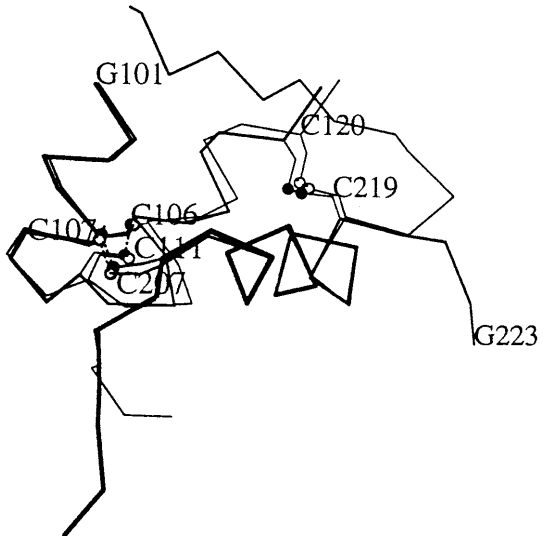


FIG. 5. Relative motion among the α-helices and S—S bonds. DHPI molecule 1 (boldface lines) and 2Zn insulin molecule 1 (regular lines) are superposed in main chains of B9–B19. The sulfur atoms are shown as circles while the S—S bonds are indicated with dotted lines. Residues are labeled as in Fig. 1. [This figure was produced using MOLSCRIPT (28).]

Table 4. Relative motion among three $\alpha$-helices in insulin and its analogs

| Molecule | A1–A8 | A12–A18 |
|---|---|---|
| DHPI(1) | | |
| $\theta$, ° | 0 | 0 |
| $t$, Å | 0 | 0 |
| DHPI(2) | | |
| $\theta$, ° | 5.20 | 5.82 |
| $t$, Å | 2.07 | 2.41 |
| INS | | |
| $\theta$, ° | 2.24 | 6.04 |
| $t$, Å | 0.99 | 3.56 |
| DPI | | |
| $\theta$, ° | 7.20 | 7.14 |
| $t$, Å | 3.40 | 3.04 |
| DHI | | |
| $\theta$, ° | 5.99 | 5.72 |
| $t$, Å | 1.90 | 1.57 |
| DesB1-B2DPI | | |
| $\theta$, ° | 5.85 | 3.49 |
| $t$, Å | 2.68 | 0.79 |

Based on the main chain superposition of insulin and insulin analogs in $\alpha$-helix B9–B19, the rotation ($\theta$) and translation ($t$) of the other two $\alpha$-helices relative to B9–B19 of DHPI(1) are computed by superposition facility in X-PLOR (26). DesB1–B2DPI, des(B1–B2) despenta peptide (B26–B30) insulin. INS represents 2Zn insulin molecule 1, while DHPI(1) and DHPI(2) represent the DHPI molecules 1 and 2, respectively.

N and C termini of B-chain as shown in Fig. 6. Maximal shifts of main chain atoms in the N and C termini reach 10 Å and 13 Å, respectively. Despite considerable flexibility in N-terminal B-chain (B1–B4), structural conservation is observed in the region consisting of B5–B6 and A6–A11, and there are three hydrogen bonds in 2Zn insulin and in truncated insulin analogs as shown in Table 5. In fact, in rebuilding the model of DHPI, if B1–B4 followed the conformation of DPI, close contacts would occur between Phe$^{B1}$ of molecule 1 and Tyr$^{B16}$ of symmetry-related molecule 2. The lattice packing force drives the B1–B4 to take a completely different conformation from DPI with rotation ($\approx$180°) in the $\psi$ torsion angle of Gln$^{B4}$. It seems that the forces to maintain the local structure in B5–B6 and A6–A11 are strong enough to resist any perturbation from lattice packing forces in the crystal structures of T-like forms available to date. It is also noticeable that this region makes a relatively slight thermal motion compared with the molecule core in the case of DHPI. The average B-factors for B5–B6, A6–A11, and whole molecule are 9.40 Å$^2$, 7.77 Å$^2$, and 13.42 Å$^2$, respectively, in DHPI molecule 1, compared with 21.87 Å$^2$, 22.19 Å$^2$, and 22.38 Å$^2$ in 2Zn insulin molecule 1. Taking into account a strong propensity of B1–B8 to undergo conformational adjustment and reach *R* state, another stable state in insulin (32, 33, 34), structural conservation in the region of B5–B6 and A6–A11 in T form indicates that a certain energy is required to induce the transformation. It suggests the possibility that, under the physiological condition when insulin brings about its biological effects as a monomer, the regional structures of B5–B6 and A6–A11 exhibit the same conformation as that in the T-state crystal. With evidence found to demonstrate the importance of B5–B6 in determining the activity of insulin (35), the structural feature of B5–B6 and A6–A11 may also implicate its special role in insulin-mediated signal transduction, not excluding its participation in direct binding with insulin receptor.

**The Role of Phe$^{B24}$.** Current studies have emphasized the role of invariant Phe$^{B24}$ in insulin receptor binding. Substitution of Ser or Leu at position B24 will cause markedly reduced binding potency of mutants, and deletion of Phe$^{B24}$ will make DHPI molecule virtually inactive. On the other hand, B24 can tolerate the replacement of D-amino acid residues. To manifest the role of Phe$^{B24}$ in the interaction of insulin with its receptor, a series of truncated insulin analogs was designed, and their crystal structures were determined. Whereas the three $\alpha$-helices remain stable, a profound conformational change is

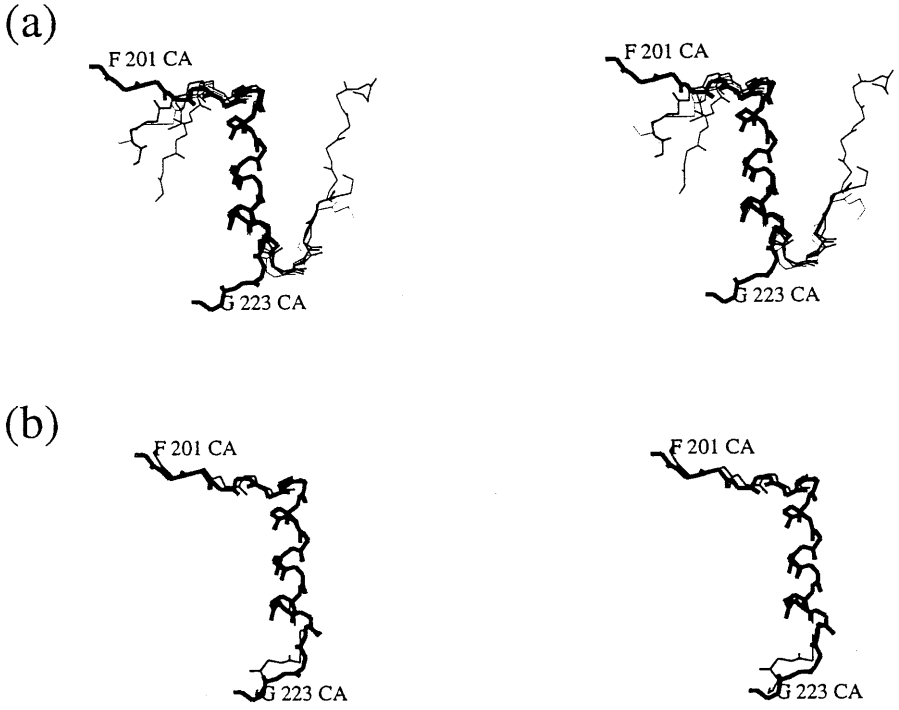


FIG. 6. Structural comparison of DHPI with insulin and insulin analogs. (*a*) Main chain superposition of B-chains of DHPI molecule 1 (boldface lines) and 2Zn insulin, DPI, DHI, and des (B1–B2) despentapeptide (B26–B30) insulin (regular lines). Only B9–B19 were used to calculate the superposition matrices. (*b*) Similar comparison of DHPI molecule 1 (boldface lines) and molecule 2 (regular lines). Residues are labeled as in Fig. 1. [This figure was drawn with the program FRODO (27).]

Table 5. Hydrogen bonds between A6–A9 and B5–B6 in insulin and its analogs

| Bonding atoms | INS | DPI | DHI | DesB1–B2DPI | DHPI(1) | DHPI(2) |
|---|---|---|---|---|---|---|
| $Cys^{A6}O$–$Leu^{B6}N$ | 2.78 | 2.80 | 2.85 | 3.00 | 2.92 | 2.84 |
| $Cys^{A7}O$–$His^{B5}ND1$ | 2.83 | 2.87 | 2.48 | 2.91 | 2.67 | 2.86 |
| $Ser^{A9}O$–$His^{B5}ND1$ | 3.03 | 2.86 | 2.70 | 3.08 | 3.58 | 2.94 |

Values represent the distances in Å. The molecules adopt the same names as in Table 4. Des(B1–B2)DPI, dis(B1–B2) despenthapeptide (B26–B30) insulin; INS, 2Zn insulin.

observed, with β-turn lost in the B-chain C terminus in DHPI. Compared with DHI, it seems that the potential hydrogen bonds between $Gly^{B20}$-O–$Gly^{B23}$-N and $Asn^{A21}$-O—$Arg^{B22}$-NE in DHI are not strong enough to constrain the B21–B23 rigidly to the hydrophobic core in DHPI. As evidence is found to support the hypotheses that the side chain of $Phe^{B25}$ may initiate a structural adjustment in the main chain nearby and induce the direct contact of the main chain in B24–B25 with receptor (9, 13, 14), a certain energy is required to maintain a high-affinity binding state in the region during the structural adjustment in native insulin. Detailed examinations at crystal structures of 2Zn insulin and insulin analogs with high receptor binding potency find that the side chain of B24 lies against the hydrophobic surface with many hydrophobic interactions between the aromatic ring of B24 and the side chains of $Val^{B12}$, $Leu^{B15}$, $Tyr^{B16}$, and $Cys^{B19}$ in these structures. Comparatively, no evidence has yet been found to prove the contribution of the main chain near $Phe^{B24}$ to the maintenance of a high-affinity binding state in B-chain C terminus. We can therefore infer that $Phe^{B24}$, mainly the aromatic ring, may play a leading role in maintaining the β-turn structure in the C terminus of B-chain. Moreover, β-turn is found to be a conservative structure in insulin and insulin analogs with high potency, and it tethers the C-terminal B-chain domain to the hydrophobic core and constructs a possible receptor-binding surface (5, 36). The dissociation of β-turn in DHPI may be a chief cause responsible for the tremendous loss of activity of the analog. This may also account for 0.98% and 0.2% of binding affinity in [$Gly^{B24}$-α-carboxamide]DPI and [$Gly^{B24}$,$Gly^{B25}$-α-carboxamide]DPI compared with 147% and 22% in their parent analogs, [$Phe^{B24}$,$Phe^{B25}$-α-carboxamide]-DPI and [$Phe^{B24}$,$Gly^{B25}$-α-carboxamide]DPI, respectively (12), though their crystal structures are not available to date. Taken together, the results presented here document the leading role of the side chain of $Phe^{B24}$ in maintaining the β-turn (B20–B23) in insulin and provide evidence for the importance of β-turn in maintaining a high-affinity binding state in insulin when bound to receptor.

This work is supported by the National Natural Science Foundation of China and the Chinese Academy of Sciences (Grant KJ85-04-10).

1. Olefsky, J., Saekow, M., Tager, H. & Rubenstein, A. (1980) *J. Biol. Chem.* **255,** 6098–6105.
2. Tager, H., Thomas, N., Assoian, R., Rubenstein, A., Saekow, M., Olefsky, J. & Kaiser, E. T. (1980) *Proc. Natl. Acad. Sci. USA* **77,** 3181–3185.
3. Shoelson, S., Haneda, M., Blix, P., Nanjo, A., Sanke, T., Inouye, K., Steiner, D., Rubenstein, A. & Tager, H. (1983) *Nature (London)* **302,** 540–543.
4. Wang, C. C. & Liang, D. C. (1985) *Chin. Biochem. J.* **1,** 9–12.
5. Liang, D. C., Chang, W. R. Zhang, J. P. & Wan, Z. L. (1992) *Sci. China Ser. B* **35,** 547–557.
6. Murray-Rust, J., Mcleod, A. N., Blundell, T. L. & Wood, S. P. (1992) *BioEssays* **14,** 325–331.
7. Hua, Q. X., Shoelson, S. E. & Weiss, M. A. (1992) *Biochemistry* **31,** 11940–11951.
8. Spoden, M, Gattner, H.-G., Zahn, H. & Brandenberg, D. (1995) *Int. J. Pept. Protein Res.* **46,** 221–227.
9. Nakagawa, S. H. & Tager, S. H. (1986) *J. Biol. Chem.* **261,** 7332–7341.
10. Mirmira, R. G. & Tager, S. H. (1989) *J. Biol. Chem.* **264,** 6349–6354.
11. Mirmira, R. G. & Tager, S. H. (1991) *Biochemistry* **30,** 8222–8229.
12. Nakagawa, S. H. & Tager, H. S. (1993) *Biochemistry* **32,** 7237–7243.
13. Nakagawa, S. H., Jogansen, N. L., Madsen, K., Schwartz, T. W. & Tager, H. S. (1993) *Int. J. Pept. Protein Res.* **42,** 578–584.
14. Wollmer, A., Gilge, G., Brandenburg, D. & Gattner, H.-G. (1994) *Biol. Chem. Hoppe-Seyler* **375,** 219–222.
15. Chu, S. C. (1987) *Acta Biochim. Biophys. Sin.* **19,** 99–104.
16. Dai, J. B., Lou, M. Z., You, J. M. & Liang, D. C. (1987) *Sci. Sin. Ser. B* **30,** 55–65.
17. Chang, W. R., Jiang, T., Ren, Z., Wan, Z. L., Xu, Y. B., Liang, D. C., Zhu, S. Q. & Zhang, Y. S. (1995) *Sci. China Ser. B* **38,** 1904–1100.
18. Lu, Z. X. & Yu, R. H. (1980) *Sci. Sin.* **23,** 1592–1596.
19. Chang, W. R., Xie, D. L., Liang, D. C., Ru, Z. X. & Yu, R. H. (1982) *Sci. Sin. Ser. B* **25,** 385–388.
20. Matthew, B. W. (1968) *J. Mol. Biol.* **33,** 491–497.
21. North, A. C. T., Philips, D. C. & Mathews, F. S. (1968) *Acta Crystallogr. A* **24,** 315–359.
22. Steigemann, W. (1974) Ph.D. thesis (Thechische Univ., München, Germany).
23. Sakabe, N. (1983) *J. Appl. Crystallogr.* **16,** 542–547.
24. Higashi, T. (1989) *J. Appl. Crystallogr.* **22,** 9–18.
25. Navaza, J. (1994) *Acta Crystallogr. A* **50,** 157–163.
26. Brünger, A. T. (1992) X-PLOR, A System for X-Ray Crystallography and NMR (Yale Univ. Press, New Haven, CT), Version 3.1.
27. Jones, T. A. (1978) *J. Appl. Crystallogr.* **11,** 268–272.
28. Kraulis, P. J. (1991) *J. Appl. Crystallogr.* **24,** 946–950.
29. Chang, W. R., Stuart, D., Dai, J. B., Todd, R., Zhang, J. P., Xie, D. L., Kuang, B. & Liang, D. C. (1986) *Sci. Sin. Ser. B* **29,** 1273–1284.
30. Baker, E. N., Blundell, T. L., Cutfield, J. F., Cutfield, S. M., Dodson, E. J., Dodson, G. G., Hodgkin, D. C., Hubbard, R. E., Isaacs, N. W., Reynolds, C. D., Sakabe, K., Sakabe, N. & Vijayan, M. (1988) *Philos. Trans. R. Soc. London B* **319,** 369–456.
31. Rossmann, M. G. & Blow, D. M. (1962) *Acta Crystallogr.* **15,** 24–31.
32. Bentley, G., Dodson, E., Dodson, G., Hodgkin, D. & Mercola, D. (1976) *Nature (London)* **261,** 166–168.
33. Smith, G. D., Swenson, D. C., Dodson, E. J., Dodson, G. G. & Reynolds, C. D. (1984) *Proc. Natl. Acad. Sci. USA* **81,** 7093–7097.
34. Derewenda, U., Derewenda, Z., Dodson, E. J., Dodson, G. G., Reynolds, C. D., Smith, G. D., Sparks, C. & Swenson, D. (1989) *Nature (London)* **338,** 594–596.
35. Nakagawa, S. H. & Tager, H. S. (1991) *J. Biol. Chem.* **266,** 11502–11509.
36. Liang, D. C., Chang, W. R. & Wan, Z. L. (1994) *Biophys. Chem.* **50,** 63–71.